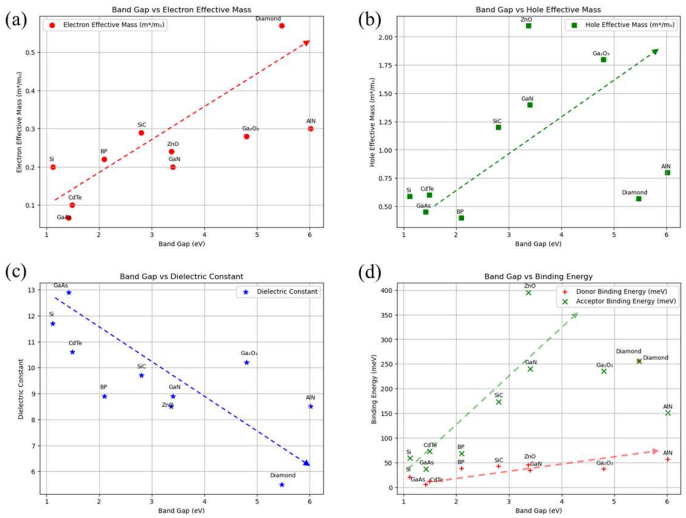

Figure 1. (a) Electron and (b) hole effective mass of materials with varying bandgaps, showing an increasing trend with bandgap. (c) Dielectric constant of semiconductor materials, which decreases as bandgap increases. (d) Donor and acceptor binding energies calculated using the hydrogen model. High acceptor binding energies present challenges for p-type doping.

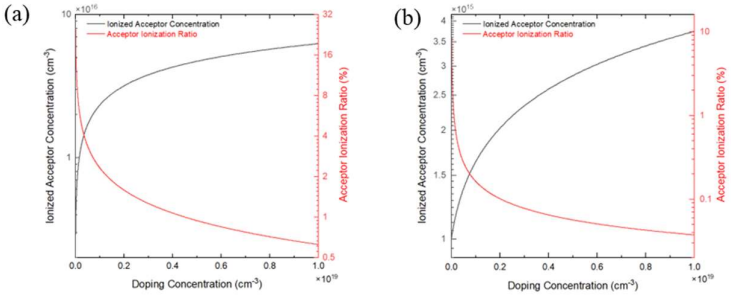

Figure 2. For (a) CdTe and (b) GaN with a background donor concentration of 10^{15} cm^{-3}, their calculated ionized acceptor concentration and acceptor ionization ratio as a function of doping concentration.

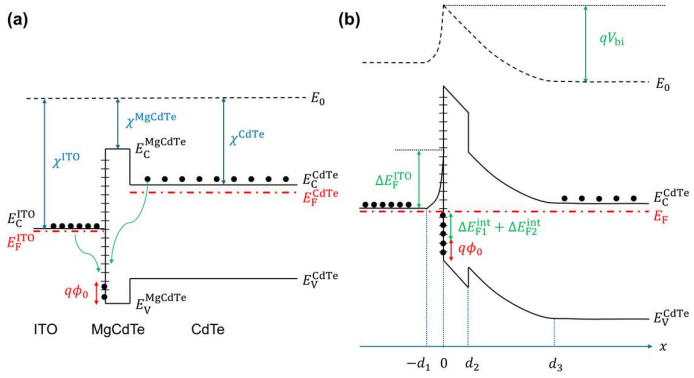

Figure 3. (a) Schematic band alignment before spatial charge transfer. The arrows indicate the charger transfer trends. (b) Band diagram at equilibrium after the charge transfer. The diagram shows a back-to-back N$^+$-p-n junction (N$^+$: heavily doped wide bandgap materials), while the N$^+$-p junction behaves as a tunnel junction due to high electron concentration in the ITO layer. Thus, the ITO/MgCdTe interface here acts as a hole-selective contact.

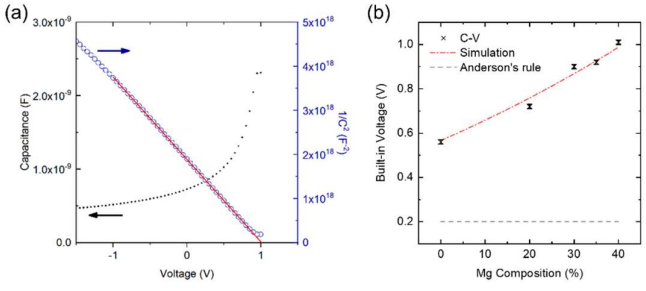

Figure 4. (a) *C-V* measurement results of a device with 40% of Mg in the top barrier layer. The 1.01 V V_{bi} is extrapolated by linear fitting from the $1/C^2$-V curve (red line). (b) Built-in voltage as a function of Mg composition in the top barrier layer. The V_{bi} increases linearly with Mg composition. The dashed line shows V_{bi} calculated by using Anderson's rule, which is a constant ~0.2 V, regardless of Mg composition in the top barrier layer.